JOURNAL OF MATERIALS SCIENCE **40** (2005) 2765–2773

Relation between grain boundary segregation and grain boundary character in FCC alloys

P. WYNBLATT*, ZHAN SHI
Department of Materials Science and Engineering, Carnegie Mellon University, Pittsburgh, PA 15213, USA
E-mail: pw01@andrew.cmu.edu

An analytical model of segregation at grain boundaries, which takes into account all five macroscopic parameters of grain boundary character, has been developed. The model is based on a combination of previous bond energy treatments of grain boundary energy and of segregation to free surfaces. It is tested by comparing its predictions against previous computations of segregation to symmetrical twist grain boundaries in simple fcc alloys obtained by Monte Carlo simulations in conjunction with embedded atom method potentials. The comparison shows good agreement with the previous computer simulations. Examples of model predictions in the case of asymmetric grain boundaries are also provided.

1. Introduction

It is now possible to characterize vast sets of grain boundaries (GB's) with respect to the five macroscopic degrees of freedom (DoF's) of GB character by automated experimental techniques. Whereas computer simulation remains the most reliable approach for predicting GB properties, this approach cannot easily be used to predict the behavior of GB's over the vast 5-dimensional space represented by the five DoF's. Thus, there is a need for analytic techniques that are capable of calculating GB properties. This paper represents an attempt to develop an analytical model of GB segregation, as a function of the five DoF's.

Interfacial segregation in a multi-component system refers to the enrichment (or depletion) of interfaces with respect to one or more components relative to the bulk composition [1]. This phenomenon has been widely studied from both experimental and theoretical perspectives, because of its influence on many important materials properties. Our approach follows the approximate statistical mechanical treatments of segregation originally developed by McLean [2], whose results may be expressed in the case of a binary solution as:

$$\frac{x_s}{1-x_s} = \frac{x}{1-x}\exp\left(-\frac{\Delta G_{\text{seg}}}{RT}\right) \qquad (1)$$

where x and x_s are the atom fractions of the segregating component in the bulk and at the interface, respectively, R and T are the gas constant and absolute temperature, and ΔG_{seg} is the free energy of segregation. For a substitutional solid solution, the latter quantity represents the free energy change associated with the exchange of an atom of the segregating species located in the bulk with an atom of the other species located at the interface [3]. Since many binary alloy systems may reasonably be approximated as regular solutions, the entropy of segregation is often neglected, and the free energy of segregation is set equal to the enthalpy of segregation, ΔH_{seg}. As will be shown below, ΔH_{seg} is a function of both x and x_s. If an expression for the enthalpy of segregation is available, it may then be used in Equation 1 to compute the interfacial composition as function of bulk composition and temperature.

Several approaches have been developed to evaluate the enthalpy of segregation. Here, the general approach used is one in which the total enthalpy of segregation is taken to consist of a sum of a chemical (or bond energy) contribution and an elastic strain energy contribution [3].

Specifically, we propose a model to calculate the equilibrium composition of a grain boundary characterized by five macroscopic DoF's. Thus far, no model with such capabilities has been developed. We use two previous pieces of work as a basis for the model, (a) a multi-layer surface segregation model [4] and (b) a semi-empirical grain boundary energy model written in terms of the five macroscopic DoF's [5]. The latter has recently been used with some considerable success to rationalize the results of GB wetting experiments in polycrystalline alloys. Both approaches have relied heavily on the prior work of Lee and Aaronson [6, 7]. In this paper, we develop the GB segregation model and test it by comparing its predictions against the results of computer simulations of GB composition obtained for sets of twist boundaries in four simple alloys.

*Author to whom all correspondence should be addressed.

2. Multi-layer surface segregation

We begin with a review of the surface segregation model. This is due to Lee and Aaronson [6, 7], as modified by Steigerwald *et al*. [4], and is suitable for the description of segregation to a surface of orientation (*hkl*) in a binary substitutional solution. In the model, the indices of the terminating planes must be chosen such that $h \geq k \geq l$ and reduced to the lowest integers. The composition of the ith layer in the vicinity of the (*hkl*) surface has the same form as that of Equation 2 written in the regular solution approximation, namely:

$$\ln \frac{x^i}{1-x^i} = \ln \frac{x}{1-x} - \frac{\Delta H^i_{\text{seg}}}{RT} \tag{2}$$

where x^i and x are the atomic fractions of the segregating species in the ith atomic layer and in the bulk, respectively, and ΔH^i_{seg} is the enthalpy of segregation to the ith layer, which includes both chemical and elastic energy terms. Near-surface planes are identified by an index i, where $i = 1$ identifies the outer-most atom plane. It is also necessary to define a second index, j, which counts the planes from any given plane i. These indices are illustrated in the schematic of Fig. 1 and are also explained in greater detail in the paper of Lee and Aaronson [6].

We consider an AB substitutional solid solution in which the solute species is taken to be component B. For convenience, we also assume that the solute corresponds to the segregating species. Although the solute is often the segregating species in solid solutions, this is not invariably the case. However, in the event that the solvent is the segregating species, the enthalpy of segregation for the solute calculated by the model will turn out to be positive. From Equation 2, it can be seen that a positive enthalpy will produce a lower ith layer concentration of solute than in the bulk, thus correctly predicting solvent segregation for such a case.

For an fcc crystal surface terminated by a plane (*hkl*), the enthalpy of segregation to the ith layer may readily be computed from the bond energy change associated with the exchange of a segregating species atom in the bulk with an atom of the other species located in layer i. In addition to the bond energy changes, the exchange of a solute atom in the bulk with a solvent atom in the ith atomic layer will lead to a change in the elastic strain energy associated with the solute atom. This is because part of the elastic energy of the solute atom in the bulk will be relieved as it comes closer to the surface. The decrease in elastic strain energy of a solute atom in the ith layer, due to its vicinity to the surface, will be denoted as ΔE^i_{el}, defined as a positive quantity. Details of the calculation of this quantity will be provided later. In the mean time, we will include it in the overall enthalpy of segregation.

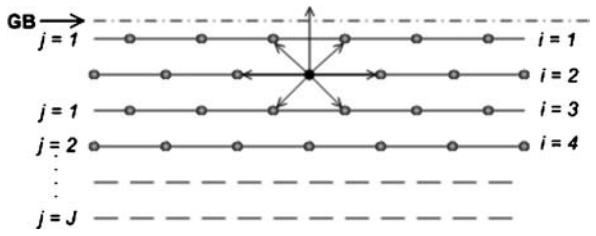

Figure 1 Schematic of a GB illustrating the definition of the index j for a value of $i = 2$. The arrows show the bonds of an atom in the ith layer from the GB plane.

Summing over bond and elastic strain energy terms yields the segregation enthalpy for a free surface [4]:

$$\Delta H^i_{\text{seg}} = 2\omega\left[zx - z^i x^i - \sum_{j=1}^{J} z^j x^{i+j} - \sum_{j=1}^{i-1} z^j x^{i-1} - \frac{1}{2}\sum_{j=i}^{J} z^j\right] - \frac{1}{2}(\varepsilon_{BB} - \varepsilon_{AA})\sum_{j=i}^{J} z^j - \Delta E^i_{el} \quad \text{for } i \leq J \tag{3a}$$

$$\Delta H^i_{\text{seg}} = 2\omega\left[zx - z^i x^i - \sum_{j=1}^{J} z^j (x^{i+j} + x^{i-j})\right] - \Delta E^i_{el} \quad \text{for } i > J \tag{3b}$$

where ω is the regular solution constant is given by:

$$\omega = \varepsilon_{AB} - \frac{1}{2}(\varepsilon_{AA} + \varepsilon_{BB}) \tag{4}$$

Here z^i is the number of nearest neighbors of an atom in the ith layer which also lie in the ith layer, and z^j is the number of nearest neighbors of an atom in the ith layer which lie in the jth layer, and the total coordination of an atom in the bulk is given by: $z = z^i + 2\sum_{j=1}^{J} z^j$. ε_{AA} and ε_{BB} are the energies of bonds between pairs of like-atoms, and ε_{AB} is the bond energy of an unlike pair (all taken to be negative quantities). The maximum value of j is denoted by J, and represents the farthest plane containing nearest neighbors of atoms in the ith layer. It is defined by $J = (h + k)/2$ for h, k, l odd, and $J = (h + k)$ for h, k, l mixed.

3. Derivation of the GB segregation model

The enthalpy of grain boundary segregation can be calculated by the same procedure. However, it is necessary to adjust atom coordination to the environment of a grain boundary. For an atom in the ith layer of a surface, the number of out of plane bonds directed towards the surface is $\sum_{j=1}^{J} z^j$. Of these, $\sum_{j=1}^{i-1} z^j$ are connected to neighbors, and the number of broken bonds is $\sum_{j=i}^{J} z^j$. When a GB is created by bringing together two crystals terminated by (*hkl*) surfaces at some arbitrary twist angle, then some of the broken bonds will reconnect across the boundary to produce a decrease in the number of broken bonds. We define a parameter P to represent the fraction of reconnected broken bonds in the near-boundary region when the plane (*hkl*) terminates one side of a GB. Thus, for an atom in the ith layer on one side of the boundary, $P\sum_{j=i}^{J} z^j$ bonds are connected to the surface of the crystal on the other side of the grain boundary, and the remaining $(1 - P)\sum_{j=i}^{J} z^j$ bonds are still broken.

We now compute the bond energy change associated with the exchange of a solute (B) atom in the bulk with

a solvent (A) atom in the ith layer. For clarity, this is performed in four steps.

Step 1. The bond energy change associated with removing a B atom from the bulk is given by:

$$E_1 = -\left[z^i + 2\sum_{j=1}^{J} z^j\right][x\varepsilon_{BB} + (1-x)\varepsilon_{AB}] \quad (5a)$$

Step 2. Replacing this B atom in the ith near-GB layer produces the following bond energy change:

$$\begin{aligned} E_2 = &+ z^i[x^i\varepsilon_{BB} + (1-x^i)\varepsilon_{AB}] \\ &+ \sum_{j=1}^{i-1} z^j[\varepsilon_{BB}x^{i-j} + \varepsilon_{AB}(1-x^{i-j})] \\ &+ \sum_{j=1}^{J} z^j[x^{i+j}\varepsilon_{BB} + (1-x^{i+j})\varepsilon_{AB}] \\ &+ P\sum_{j=i}^{J} z^j[x'\varepsilon_{BB} + (1-x')\varepsilon_{AB}] \end{aligned} \quad (5b)$$

where x' is some suitable average of the near-interface composition of the crystal on the other side of the boundary.

Step 3. Removing an A atom from the ith near-GB layer changes the bond energy by:

$$\begin{aligned} E_3 = &- z^i[x^i\varepsilon_{AB} + (1-x^i)\varepsilon_{AA}] \\ &- \sum_{j=1}^{i-1} z^j[x^{i-j}\varepsilon_{AB} + (1-x^{i-j})\varepsilon_{AA}] \\ &- \sum_{j=1}^{J} z^j[x^{i+j}\varepsilon_{AB} + (1-x^{i+j})\varepsilon_{AA}] \\ &- P\sum_{j=i}^{J} z^j[x'\varepsilon_{AB} + (1-x')\varepsilon_{AA}] \end{aligned} \quad (5c)$$

Step 4. Finally, replacing an A atom in the bulk yields:

$$E_4 = +\left[z^i + 2\sum_{j=1}^{J} z^j\right][x\varepsilon_{AB} + (1-x)\varepsilon_{AA}] \quad (5d)$$

Summing over the four steps yields an expression similar to Equation 3a for the case $i \leq J$, but with correction terms that account for the larger coordination of atoms near the grain boundary, as well as interaction terms across the grain boundary.

$$\begin{aligned} \Delta H^i_{\text{seg}} = 2\omega\Bigg[& zx - z^i x^i - \sum_{j=1}^{J} z^j x^{i+j} - \sum_{j=1}^{i-1} z^j x^{i-j} \\ & - P\sum_{j=i}^{J} z^j x' - \frac{1}{2}(1-P)\sum_{j=i}^{J} z^j \Bigg] \\ & - \frac{1}{2}(1-P)(\varepsilon_{BB} - \varepsilon_{AA})\sum_{j=i}^{J} z^j - \Delta E^i_{el} \end{aligned} \quad (6a)$$

For atoms in layers $i > J$, the enthalpy of segregation is unchanged from Equation 3b, i.e.:

$$\Delta H^i_{\text{seg}} = 2\omega\left[zx - z^i x^i - \sum_{j=1}^{J} z^j(x^{i+j} + x^{i-j})\right] - \Delta E^i_{el}$$

4. GB energy model

Here we summarize the GB energy model [5], which is also used as a basis for the present segregation model. A GB can be created by joining two crystals together. Four of the five DoF's of the GB can be determined by specifying the two crystallographic planes $(hkl)_1$ and $(hkl)_2$, which terminate the adjacent crystals on either side of the grain boundary. The fifth DoF is defined by the twist angle, ϕ, of the two crystals with respect to each other about an axis perpendicular to the GB plane. Wolf [8–10] has performed computer simulations on grain boundary energy as a function of twist angle for boundaries having specified terminating planes. That work has shown that the grain boundary energy is essentially constant over most of the twist angle range except for cusps at certain specific values. This constant value will be referred to as the plateau value, as illustrated schematically in Fig. 2.

Lee and Aaronson [6] have developed a broken bond model which allows the calculation of the energy of a surface of orientation (hkl) in a pure (one component) material:

$$\gamma^s_{(hkl)} = \frac{\alpha\varepsilon}{a^2\sqrt{h^2+k^2+l^2}}\sum_{i=1}^{J}\sum_{j=i}^{J} z_j \quad (7a)$$

where α is a constant which adopts values of 2 for (hkl) all odd and of 1 for (hkl) mixed, ε is the energy of a broken bond, and a is the lattice constant. The double sum on z_j represents the number of broken bonds at a surface of orientation (hkl), as described in more detail by Lee and Aaronson [6].

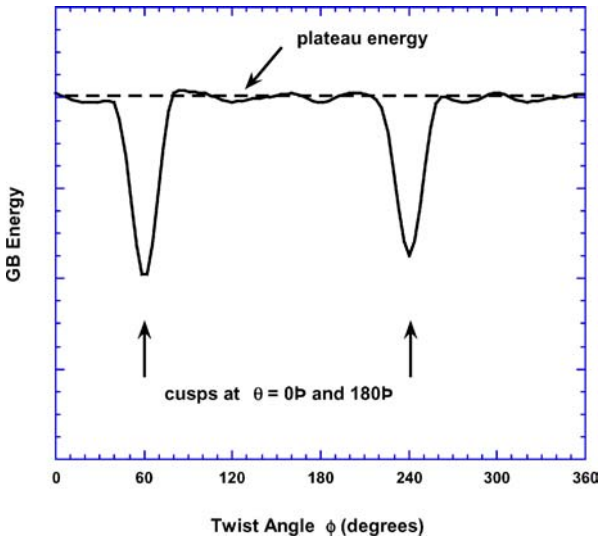

Figure 2 Schematic illustration of the energy of a twist GB vs. twist angle. Note that the energy is essentially constant over most of the twist angle range at a value referred to as the "plateau energy", except for cusps which occur at particular values of twist angle (see Section 4).

The Lee and Aaronson model has been adapted to GB's by Wynblatt and Takashima [5]. For the case of a GB terminated by two planes of identical (*hkl*), the (approximately constant) plateau GB energy is written:

$$\gamma^M_{(hkl)} = \frac{2\alpha\varepsilon}{a^2\sqrt{h^2+k^2+l^2}} V^M_{(hkl)} \sum_{i=1}^{J}\sum_{j=i}^{J} z_j \qquad (7b)$$

Here we use the superscript M as a reminder that these terms refer to the maximum (i.e. plateau) values. The differences between Equations 7a and b include a factor of 2 in 7b, which reflects the fact that a GB consists of two crystals each terminated at a surface, and a factor,

$$V^M_{(hkl)} = F[g_t(1-f_{sk}) + f_{sk}] \qquad (8)$$

which represents the fraction by which the number of broken bonds of the two surfaces is reduced upon creating a grain boundary by joining the two crystals with (*hkl*) surfaces. F is an adjustable parameter, and the quantities g_t and f_{sk} are related to surface roughness, as discussed in more detail below. $V^M_{(hkl)}$ can also be considered to represent a free-volume-like parameter for the boundary, such that the smaller the free volume, the lower the number of broken bonds across the GB.

Free volume is an important property of GB's, as has been demonstrated in the computer simulations of Wolf [8–10], which showed that GB energy is essentially proportional to free volume. This trend was used as one of two guiding criteria in the formulation of the GB energy model of ref. [5]. The free volume is also used in the present segregation model to evaluate both the parameter P, as well as the solute strain energy term, ΔE^i_{el}. We therefore provide a detailed explanation the origin of this term in Section 4.1 below.

The scheme of Van Hove and Somorjai [11] can be used to synthesize an (*hkl*) surface from microfacets, which represent terraces, steps and kinks. Thus, any fcc (*hkl*) surface, which lies within the standard stereographic triangle ($h \geq k \geq l$), can be decomposed into (111), (11$\bar{1}$) and (100) microfacets. For this choice of microfacet orientations, the number of atoms associated with each microfacet is given by:

$$n_{(111)} : n_{(11\bar{1})} : n_{(100)} = (k+l) : (k-l) : (h-k) \quad (9a)$$

If the three values of $n_{(hkl)}$ are ranked in magnitude, the largest value will give the relative number of atoms associated with terrace sites, the middle value will be the number of atoms associated with step sites and the lowest value will be the number of atoms in kink sites, i.e.:

$$\begin{aligned} n_{\min} : n_{\text{mid}} : n_{\max} : (n_{\min} + n_{\text{mid}} + n_{\max}) \\ = \textit{kink atoms} : \textit{step atoms} : \textit{terrace} \\ \textit{atoms} : \textit{total atoms} \end{aligned} \qquad (9b)$$

The underlying concept in formulating the free-volume-like parameter, $F[g_t(1-f_{sk}) + f_{sk}]$, is that the "rougher" the two surfaces which adjoin the GB, the larger the free-volume. g_t (where t stands for {111} or {100}) is intended to represent the roughness of the two possible types of terrace. Values of g_t corresponding to the fcc structure have been obtained previously [5], by demanding that the GB energy be proportional to free-volume. (These values are $g_{\{111\}} = 0.47$ and $g_{\{100\}} = 0.62$). f_{sk} is the fraction of surface atoms associated with steps and kinks, computed from Equation 9b. The larger f_{sk}, the larger the roughness, and hence the larger the free volume. The term, $g_t(1-f_{sk})$, is the terrace contribution to the roughness, and declines as the overall roughness of the surface, f_{sk}, increases.

Finally, we define F as an adjustable parameter, which may be used to scale the grain boundary energy to a known surface energy. When only relative grain boundary energies are required, the parameter F may be omitted. However, for the purposes of evaluating GB composition, a realistic value of F needs to be included.

As shown previously [5], the inclusion of the free-volume-like term of Equation 8 into the expression for GB energy (Equation 7b) leads to proportionality between GB energy and free volume, in spite of the complex dependence of $V^M_{(hkl)}$ on the structure of an (*hkl*) surface. Thus, in this regard, the GB energy model is consistent with Wolf's GB computer simulations [8–10]. Another important result of those simulations was used as a second guiding principle in the formulation of the GB energy model. The simulations showed that the energy of a GB terminated by two surfaces of different (*hkl*) varies linearly with (but is not proportional to) mean surface energy, $(\gamma^s_{(hkl)_1} + \gamma^s_{(hkl)_2})/2$.

Thus, for the case of GB's bounded by crystallographically different planes, the plateau energy is written simply as the arithmetic mean of two GB's, each bounded by planes of identical (*hkl*):

$$\gamma^M_{(hkl)_1(hkl)_2} = \left[\gamma^M_{(hkl)_1} + \gamma^M_{(hkl)_2}\right]/2 \qquad (10)$$

This simple form for the energy of a GB terminated by different (*hkl*) surfaces ensures that both of the results of Wolf's simulations, mentioned above, are reproduced by the GB energy model. The GB energy is linearly dependent on mean surface energy, but the proportionality between GB energy and surface energy is broken by the inclusion of the free-volume-like term. Also, the energy of a GB terminated by two different (*hkl*) planes is proportional to the free volume of the boundary, if it is expressed in an analogous manner [5]:

$$V^M_{(hkl)_1(hkl)_2} = \left[V^M_{(hkl)_1} + V^M_{(hkl)_2}\right]/2 \qquad (11)$$

i.e., the free-volume of a boundary between different planes is taken to be the arithmetic mean of the free volumes of boundaries terminated by identical planes.

In order to introduce the 5th DoF, a dependence on twist angle must be included in the energy. The energy of a general boundary is written as:

$$\gamma_{(hkl)_1(hkl)_2}(\theta) = \gamma^m_{(hkl)_1(hkl)_2} + f(\theta)\left\{\gamma^M_{(hkl)_1(hkl)_2} - \gamma^m_{(hkl)_1(hkl)_2}\right\} \qquad (12)^*$$

*Note, the version of this equation in the original paper [ref. 5] contains a misprint.

where $\gamma^m_{(hkl)_1(hkl)_2}$ and $\gamma^M_{(hkl)_1(hkl)_2}$ are GB energy minima (at cusps) and maxima (at the plateau value), respectively, for boundaries terminated on the planes $(hkl)_1$ and $(hkl)_2$. The function $f(\theta)$ is used to mimic a Read-Shockley trend in the vicinity of cusps and is approximated by [5]:

$$f(\theta) = \sin^{1/4}(\theta) \tag{13}$$

where θ is simply related to the twist angle, ϕ [12]. θ has a zero value at cusps, and corresponds to the value of twist angle, ϕ, at which steps on the GB terminating surfaces are aligned (for {100} and {111} terminating surfaces, which do not have steps, close packed rows are used). For arbitrary $(hkl)_1$ and $(hkl)_2$, cusps generally occur 180° apart. If one of the terminating planes is (111) or (100) then additional cusps will be found as a function of θ, with a periodicity of 180°/n, where $n = 3$ for (111), and $n = 2$ for (100). Thus, $f(\theta)$ provides a simple means of including the fifth macroscopic DoF in the model. For $f(\theta) = 1$, Equation 12 reduces to the plateau GB energy, $\gamma^M_{(hkl)_1(hkl)_2}$, which accounts for the variation of GB energy as a function of the other four DoF's. For $f(\theta) = 0$, Equation 12 reduces to the cusp energy.

The minimum energy at the cusps is taken to have the value:

$$\gamma^m_{(hkl)_1(hkl)_2} = \left|\gamma^M_{(hkl)_1} - \gamma^M_{(hkl)_2}\right| \tag{14}$$

Thus, the minimum cusp energy is zero for cusps at grain boundaries where the bounding (*hkl*) surfaces are identical, since the boundary energy disappears in that case. Conceptually, this form attempts to reflect the fact that more of the broken bonds from the terminating surface with the smaller broken bond density will connect to the opposite side than vice versa. Although crude, this approach has been quite successful in predicting GB energy for the purpose of identifying GB's that are wetted by a liquid phase [5].

4.1. Evaluation of *P*

The plateau value of the free-volume of a GB terminated by two different terminating planes has been defined in Equation 11. By analogy with the expression for the minimum GB energy at a cusp (Equation 14), we define the value of the minimum free-volume at a cusp as:

$$V^m_{(hkl)_1(hkl)_2} = \left|V^M_{(hkl)_1} - V^M_{(hkl)_2}\right|, \tag{15}$$

and the free-volume defined in terms of all five DoF's as:

$$V_{(hkl)_1(hkl)_2}(\theta) = V^m_{(hkl)_1(hkl)_2} + f(\theta)\left\{V^M_{(hkl)_1(hkl)_2} - V^m_{(hkl)_1(hkl)_2}\right\} \tag{16}$$

For a GB bounded by identical (*hkl*) planes, the number of bonds connected to the surface of the crystal on the other side of the boundary is corrected by a factor P compared to a free surface, as has been discussed above. Thus, including all five DoF's, the parameter P is defined as:

$$P = 1 - V_{(hkl)_1(hkl)_2}(\theta) \tag{17}$$

Since $V_{(hkl)_1(hkl)_2}(\theta)$ is a fraction, we have $P > 0$ for any GB orientation parameters. If $\theta = 0$, a maximum number of bonds will be connected across the GB, leading to a free-volume parameter of $V^m_{(hkl)_1(hkl)_2}$ by Equation 16, or to a free-volume of zero if $(hkl)_1 = (hkl)_2$, where the GB vanishes.

4.2. Evaluation of ΔE^i_{el}

The importance of the decrease in elastic strain energy of a solute atom, ΔE^i_{el}, as a driving force for GB segregation, was first suggested by McLean [2] in his seminal work on GB segregation. Indeed, McLean calculated GB compositions based on the assumption that elastic solute strain energy relief provided the only (significant) driving force for segregation to grain boundaries. In general, the strain energy associated with a misfitting segregating solute species in the bulk of the material will be partly relieved when the solute is exchanged with a solvent atom in the vicinity of an interface, thus leading to a contribution to the overall driving force. However, how large a fraction of the bulk solute strain energy can be relieved near an interface, such as a grain boundary, is still an open question. If the approximation is made that a solute atom behaves as a misfitting sphere embedded in an elastic continuum representing the matrix, then Friedel's solution for the solute elastic strain energy can be used [13]. In addition, the change in elastic energy of a misfitting sphere as it approaches a surface has been given by Eshelby [14]. Here, we choose to use these approximations, in a slightly modified form, to estimate ΔE^i_{el}.

Various approaches have been employed to make use of Eshelby's result in the context of *surface* segregation [4, 6]. There, it is convenient to use an expression that avoids the singular behavior of the Eshelby approach, by empirically approximating the relief of solute elastic strain energy as [4]:

$$\Delta E^i_{el} = E(\infty)\exp\left[-1.01\left(\frac{h^i}{r_B}\right)^{1.53}\right] \tag{18}$$

where h^i is the distance of the ith layer from the plane $i = 1$, r_B is the radius of a solute atom and $E(\infty)$ is the elastic strain energy of a solute atom in the bulk [13]:

$$E(\infty) = \frac{24\pi K_B G_A r_A r_B (r_A - r_B)^2}{4G_A r_A + 3K_B r_B} \tag{19}$$

In Equation 19, K_B is the bulk modulus of the solute species B, G_A is the shear modulus of the solvent, and r_A is the radius of a solvent atom. For $h^i = 0$, Equation 18 leads to $\Delta E^i_{el} = E(\infty)$, i.e. all of the strain energy associated with the *B*-atom in the bulk vanishes at the surface.

The magnitude of strain energy relief when a solute atom is transferred from the bulk to a GB could be

smaller than at a free surface, due to the limited free volume of a boundary. We therefore assume that only a fraction of the bulk strain energy, proportional to the 'free volume' and $f(\theta)$, is dissipated at $h^i = 0$, such that:

$$\Delta E^i_{el} = \beta V_{(hkl)_1(hkl)_2}(\theta) \cdot E(\infty) \exp\left[-1.01\left(\frac{h^i}{r_B}\right)^{1.53}\right] \quad (20)$$

where β is an adjustable proportionality constant. If $\theta = 0$, and $(\mathrm{hkl})_1 = (\mathrm{hkl})_2$, the GB vanishes and $\Delta E^i_{el} = 0$.

4.3. Principal shortcomings of the model

Although the GB energy, as formulated in Equation 12, provides a description in terms of the 5 DoF's, it does not correctly predict the energies at cusps corresponding to either symmetric or asymmetric tilt boundaries. Consider first the case of boundaries terminated by identical (hkl) planes. For an angle of $\theta = 0^\circ$, the boundary vanishes, and the model correctly predicts a zero energy. However, the energy of the cusp at $\theta = 180^\circ$, corresponding to a symmetric tilt boundary, is also predicted to be zero, instead of some finite value. For a case where the terminating planes of the boundary do not have identical (hkl), the cusps at 0° and 180° represent asymmetric tilt boundaries. The energies of these two boundaries are predicted to be finite, but identical, which need not be the case. Thus, as currently formulated, the model is not able to correctly predict the energies of tilt boundaries, or their corresponding free-volumes. This shortcoming could readily be addressed by assigning some arbitrary energies (or free volumes) to the cusps at angles of 0° and 180° (e.g. some specified fraction of the plateau values). However, we have chosen to avoid additional adjustable parameters, since tilt boundaries account for only a small fraction of the GB orientation space, and any deficiencies in predicting their behavior is unlikely to cause serious perturbations of the overall pattern of segregation.

5. Determination of model parameters

With the expressions for the enthalpies of segregation (Equations 6a and 3b), and for the layer-by-layer compositions of each crystal (Equation 2), the compositions of the near-boundary regions of both crystals can be computed. The parameters needed for evaluation of the compositions can be obtained as described below.

In the nearest neighbor approximation, the bond energies between pairs of like-atoms can be evaluated in terms of the energies of the (100) surfaces of the pure elements, γ_A and γ_B, as:

$$\varepsilon_{AA} = -a_A^2\gamma_A/4 \quad \text{and} \quad \varepsilon_{BB} = -a_B^2\gamma_B/4 \quad (21)$$

If (100) surface energies are not available, then average surface energies may be used, since the anisotropy of the surface energy of metals is rather small.

The regular solution constant, ω may be estimated from the heat of mixing, ΔH_m, of the alloy:

$$\omega = \Delta H_m / z x_B (1 - x_B) \quad (22)$$

The near-boundary compositions of the two (hkl) surfaces of the crystals bounding the grain boundary are evaluated separately, taking the increased coordination of the atoms near the boundary into account. Since there is an interaction between the two crystal surfaces joined at the boundary, the equilibrium grain boundary composition must be computed iteratively. Some suitable average of the near-boundary composition of the grain on the other side of the boundary must be used for the variable, x', in Equation 6a. Since the compositions of layers with broken bonds are: x^i $(i = 1$ to $J)$, we may denote x' by the following average:

$$x' = P\sum_{i=1}^{J}\sum_{j=i}^{J} z^j x^i \Big/ P\sum_{i=1}^{J}\sum_{j=i}^{J} z^j \quad (23)$$

In this expression, the P's cancel, but are included here for clarity.

6. Model predictions

This model has been developed for the case of fcc binary substitutional solid solutions. There are few consistent sets of experimental measurements of grain boundary segregation over several types of grain boundaries in simple fcc solutions. Fortunately, however, there are several results available from computer simulations using the Monte Carlo method in conjunction with Embedded Atom Method (EAM) potentials. We have selected a consistent set of simulations of the composition of symmetric <100> twist boundaries from the work of Udler and Seidman [15, 16], to compare with model predictions. These authors have also conducted similar simulations on a set of <110> symmetrical tilt boundaries [17]; however, as pointed out above, the model is not able to deal with tilt boundaries without making additional arbitrary assumptions. Thus, we have focused on the results obtained on twist boundaries.

We show below the predicted GB compositions for twist boundaries in Pt-1 at%Au, Au-1 at%Pt, Pt-3 at%Ni and Ni-3 at%Pt alloys. In order to produce model predictions suitable for comparisons with simulations based on the EAM, we have evaluated the needed model parameters from the EAM values of various physical properties, given in Table I [18]. The A-A and B-B bond energies were evaluated from EAM (100) surface energies of the pure A and B components; regular solution constants were obtained from the reported EAM heats of solution for the various alloys; and the elastic moduli needed for the evaluation of elastic strain energy terms were taken from the computed EAM elastic constants, using the values of C_{44} for the shear moduli. In the case of these simple boundaries, where both crystals are terminated by (100) planes, the compositions on both sides of the boundaries are identical, and the maximum number of layers lacking complete coordination, J, is just unity. Thus, the value of x' in Equation 6a (defined in

TABLE I EAM values of physical properties used in model evaluations [18]

Physical properties	Au	Ni	Pt
Lattice constant (Å)	4.05	3.52	3.92
Bulk modulus (ergs/cm^3)	1.67	1.804	2.83
Shear modulus (C_{44}) (ergs/cm^3)	0.45	1.28	0.68
(100) Surface energy (mJ/m^2)	918	1580	1650
Heat of solution (eV)	0.07 (in Pt)	−0.25 (in Pt)	0.09 (in Au) −0.28 (in Ni)

Equation 23) is just equal to x^1, the value of the first atomic layer composition.

Calculations were performed for same boundaries as those studied by simulation, namely: 5.0° ($\Sigma = 265$), 10.4° ($\Sigma = 61$), 16.3° ($\Sigma = 25$), 22.6° ($\Sigma = 13$), 28.1° ($\Sigma = 17$), 33.9° ($\Sigma = 289$), 36.9° ($\Sigma = 5$), 41.1° ($\Sigma = 73$) and 43.6° ($\Sigma = 29$), (expressed as pairs of twist angle, and corresponding Σ value).

The GB compositions in the two papers by Udler and Seidman [15, 16] have been reported in different units. To avoid any confusion, we report model predictions in the same manner, i.e. in excess atoms/nm^2 for Pt-Au alloys, and in excess monolayers for Pt-Ni alloys. For example, in the case of excess monolayers, the segregation is calculated from:

$$\Gamma_{\text{solute}} = \sum_i (x^i - x) \tag{24}$$

where x^i is the segregant atom fraction in the ith layer and x is the bulk atom fraction. This sum must of course be taken over both sides of boundary.

The model contains two parameters, F and β, which must be adjusted in order to compare model predictions with the results of the simulations. It should be recalled that F represents the ratio of GB energy to surface energy (for the present purposes, therefore, the values of ε and a^2 in Equation 7b have been set to unity), and β represents an adjustable parameter for the maximum solute strain energy which may be relaxed in the vicinity of a boundary. These parameters were fitted so as to optimize the relationship between model predictions and the results of the simulations. This procedure yields values of $F = 0.32$ and $\beta = 3.9$. The value of F is reasonable for the case of GB's terminated by (100) surfaces. Since the value of β is almost the reciprocal of F, which enters into Equation 20 through the term $V_{(hkl)_1(hkl)_2}(\theta)$ as a simple multiplicative factor, this implies that the elastic energy of a GB is virtually independent of either β or F. In some cases, therefore, it may be possible to eliminate the adjustable parameter β.

Fig. 3 shows the GB composition, expressed as interfacial excess as a function of twist angle, obtained from the model, together with to the results of computer simulations for all four alloys. In all cases, the absolute value of the calculated segregation increases with twist angle, in agreement with the simulations. However, the model does not account for the non-monotonic variation in composition associated with certain low Σ boundaries. In the case of Fig. 3a, which illustrates the temperature dependence of segregation in Pt-1at%Au, the model predicts a decrease in the magnitude of segregation with increasing temperature, as generally expected, and in good agreement with the simulated results.

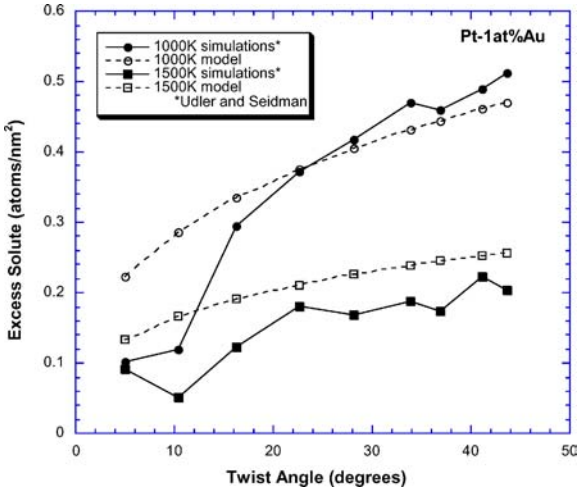

(a)

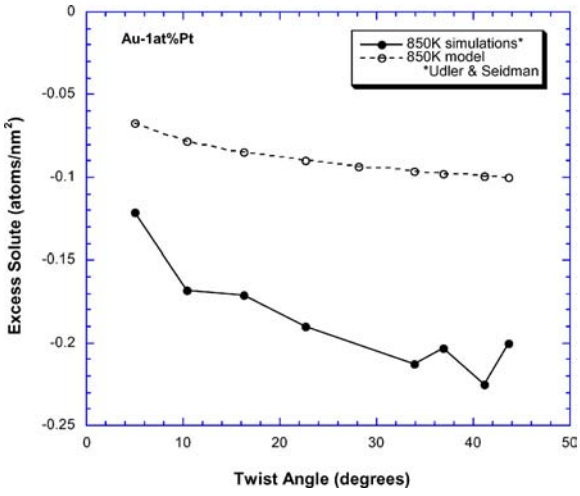

(b)

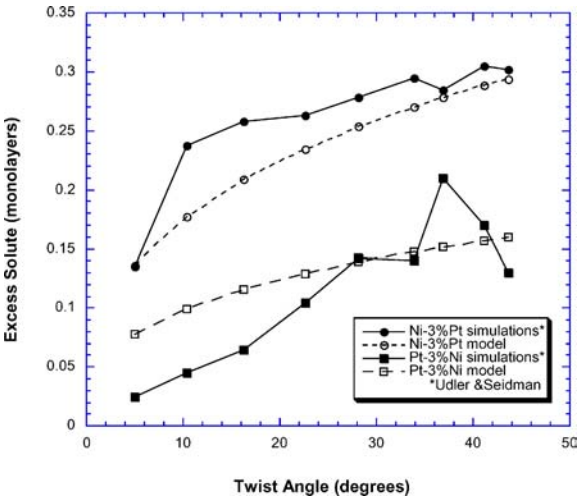

(c)

Figure 3 Comparison of model predictions for segregation to (100) symmetric twist GB's as a function of twist angle with the simulations of Udler and Seidman [15, 16]. (a) Pt-1 at%Au, (b) Au-1 at%Pt, and (c) Ni-3 at%Pt and Pt-3 at%Ni.

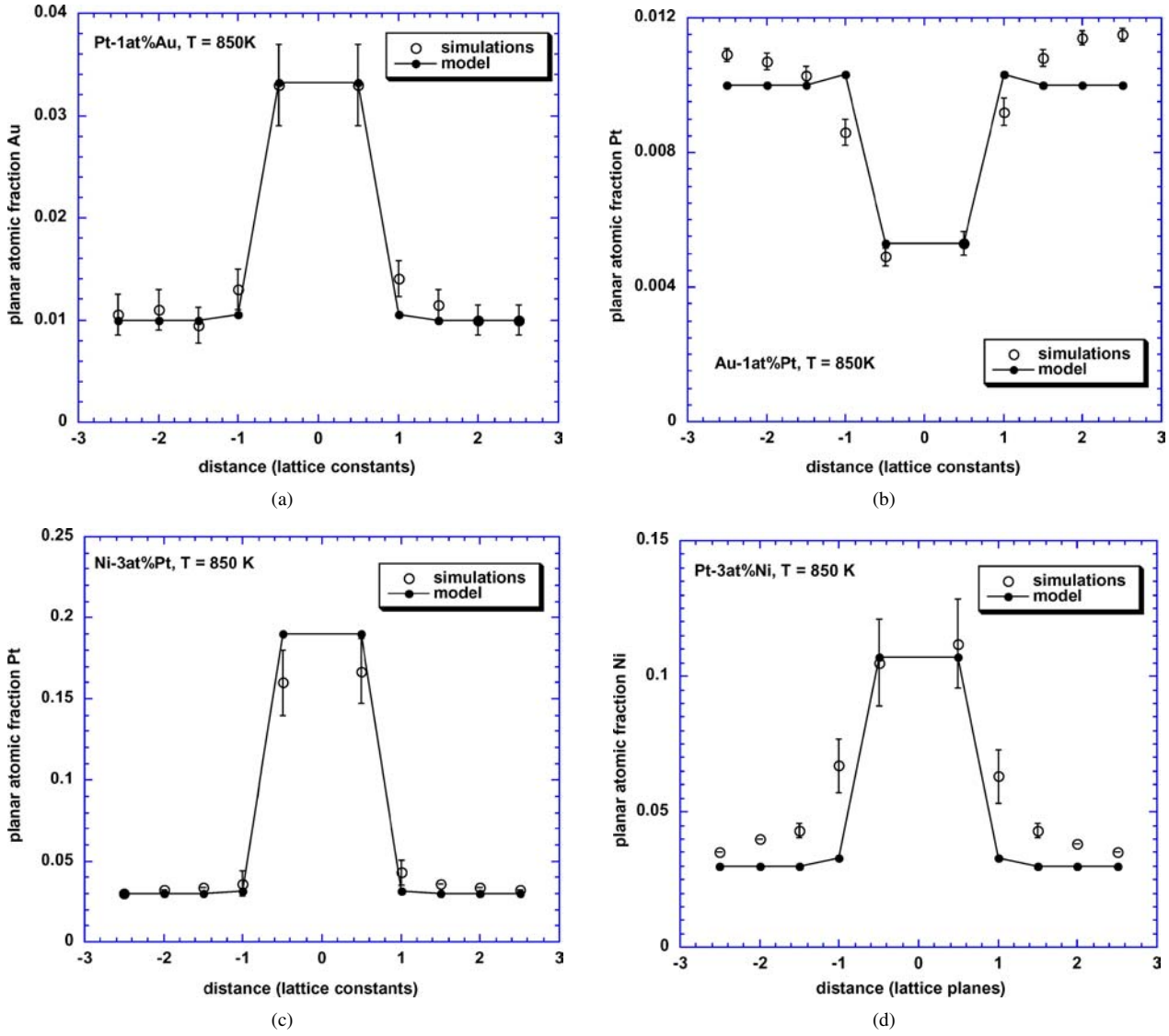

Figure 4 Comparison of model predictions of GB composition profiles with the simulations of Udler and Seidman [15, 16], at 850 K for (100) 43.6° twist boundaries in (a) Pt-1 at%Au, (b) Au-3 at%Pt, (c) Ni-1 at%Pt and (d) Pt-3 at%Ni. The spacing between the two terminating planes at the GB is arbitrary, and the line through model predictions has been added to aid the eye. Error bars on simulation results represent one standard deviation.

Fig. 3b shows the extent of segregation in the case of boundaries in a Au-1 at% Pt alloy. The results, expressed as Gibbsian excess of solute (Pt) show negative values, i.e. the model predicts segregation of the solvent (Au) in this case. This aspect of model predictions is qualitatively correct, although the predicted magnitude of segregation is lower than the results of the simulations by about a factor of about 2.

Fig. 3c displays the results obtained for both Pt–3 at%Ni and Ni-3 at%Pt alloys at a given temperature. Again, the predicted results are in good agreement with the results of the simulations.

The comparisons shown in Fig. 3 represent a reasonable test of the model in the following sense. In Pt-Au and Au-Pt alloys, the atomic sizes of the two components are approximately equal, so that the main driving force for segregation in these alloys comes about from bond energy terms, whereas the strain energy terms do not play a major role. In contrast, in Pt-Ni and Ni-Pt alloys, the surface energy term plays only a minor role, with the driving force being determined primarily by the strain energy term.

A second test of the model is provided by a comparison between the predicted layer-by-layer compositions on both sides of the boundary, for the case of 43.6° twist boundaries, in all four alloys at 850 K. Again, the agreement is remarkably good. The principal discrepancy is that segregation to the second layer, on either side of the GB, is consistently underestimated by the model. For the most part, the disagreement is small and is presumably due to the fact that, in the case of GB's terminated by (100) planes, only the first layer lacks full coordination. Under these conditions, the composition of the second layer is dictated primarily by elastic strain energy effects.

Finally, we present in Fig. 5 some predictions of the model for a number of asymmetric boundaries in the case of the Pt-1at%Au alloy at 1000 K. All of these boundaries are terminated on one side by (3 1 1) surfaces. The (3 1 1) plane lies along the (100) - (111) edge of the standard stereographic triangle. The other sides of the GB's are terminated, respectively, by the (5 3 3) surface (which also lies along the (100) - (111) edge), the (744) surface (which lies along the (110) - (111)

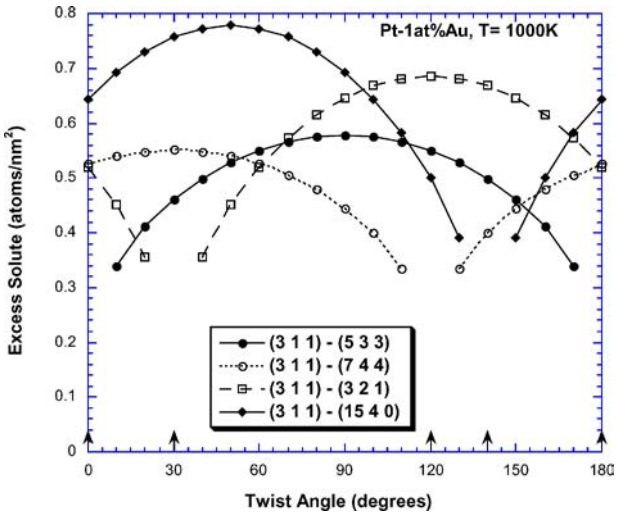

Figure 5 Examples of model predictions for asymmetric twist boundaries, as a function of twist angle, for a Pt-1 at%Au alloy at 1000 K. All the boundaries are terminated by a (311) plane on one side, and by 4 different planes on the other. Arrows indicate the location of cusps.

edge), the (15 4 0) surface (which lies along the (100) - (110) edge), and the (3 2 1) surface (which lies near the center of the stereographic triangle). Thus, these examples sample a reasonable range of possible GB orientations. When one compares the maximum values of segregation for each example, they range from about 0.55 to 0.78 excess atoms of Au per nm^2, compared to a maximum of about 0.47 in the same units for the symmetric twist boundaries of Fig. 3a.

The present comparisons with results of simulations show that in spite of obvious shortcomings, such as the use of pairwise interactions, and the assumption that bond energies are independent of atomic coordination, this simple model appears to predict reasonable trends. The advantages of an analytical framework that can be used, for example, to interpolate segregation behavior over large data sets of random polycrystalline systems should be quite valuable.

7. Summary

A simple model, which relies on nearest neighbor bond energy and elastic strain energy contributions, has been developed for investigating grain boundary segregation as a function of the five macroscopic DoF's of GB character. The model is based on the combination of a previous multi-layer model of surface segregation and a grain boundary energy model.

The model has been tested by comparing its predictions of segregation to symmetric <100> twist boundaries in Pt-1 at%Au, Au-1 at%Pt, Pt-3 at%Ni and Ni-3 at%Pt alloys, against previous computer simulations of segregation at those boundaries obtained by Monte Carlo methods in conjunction with EAM potentials. The agreement obtained in this comparison has been quite good from both qualitative and quantitative perspectives. Thus, this model should be quite valuable for the interpretation of large sets of grain boundary segregation data acquired as a function of the five macroscopic DoF's of grain boundary character.

Acknowledgement

The authors wish to acknowledge with thanks support of their research by the United States Department of Energy under Grant No. DE-FG02-99ER45779.

References

1. J. W. GIBBS, "Collected Works" (Yale University Press, New Haven, CT, 1948), Vol. 1.
2. D. MCLEAN, "Grain Boundaries in Metals" (Clarendon Press, Oxford, 1957).
3. P. WYNBLATT and R. C. KU, in "Interfacial Segregation", edited by W. C. Johnson and J. M. Blakely (American Society for Metals, Metals Park, OH, 1979) p. 115.
4. D. A. STEIGERWALD, S. J. MILLER and P. WYNBLATT, *Surf. Sci.* **155** (1985) 79.
5. P. WYNBLATT and M. TAKASHIMA, *Interf. Sci.* **9** (2001) 265.
6. Y. W. LEE and H. I. AARONSON, *Acta Metall.* **28** (1980) 539.
7. *Idem.*, *Surf. Sci.* **95** (1980) 227.
8. D. WOLF, *Acta Metall.* **37** (1989) 1983.
9. *Idem.*, *ibid.* **37** (1989) 2823.
10. *Idem.*, *Acta Metall. Mater.* **38** (1990) 791.
11. M. A. VAN HOVE and G. A. SOMORJAI, *Surf. Sci.* **92** (1980) 489.
12. P. WYNBLATT and M. TAKASHIMA, in "Proceedings of HTC-2000, edited by N. Eustathopoulos, K. Nogi and N. Sobczac, Trans. JWRI (2001), Vol 30, p. 11.
13. J. FRIEDEL, *Avan. Phys.* **3** (1954) 446.
14. J. D. ESHELBY, in "Progress in Solid Mechanics", edited by Sneddon and Hill, (North-Holland, Amsterdam, 1961) Vol. 2, p. 275.
15. D. UDLER and D. N. SEIDMAN, *Phys. Stat. Sol.* B **172** (1992) 267.
16. *Idem.*, *Acta Metal. Mater.* **42** (1994) 1959.
17. J. D. RITTNER and D. N. SEIDMAN, *Phyical Rev.* B **54** (1996) 6999.
18. S. M. FOILES, M. I. BASKES and M. S. DAW, *ibid.* **33** (1985) 7983.